International Journal of Religion
2025
Volume: 6| Number 1 | pp. 579 – 590
ISSN: 2633-352X (Print) | ISSN: 2633-3538 (Online)
ijor.co.uk
DOI: https://doi.org/10.61707/bfwj5t66

Exploring Energy Discrepancies in Steel Under Static and Dynamic Loads

Edison Gustavo Tapia Zurita[1], José Emilio Pérez Rosales[2]

Abstract

The analysis of deformation energy in the plastic range for square section rods of ASTM A36 steel subjected to bending; and, in threaded rods of ASTM A193 B7 steel subjected to tension, in both cases under static and impact load tests. In the case of static loads, the AMSLER universal testing machine with a capacity of 10 tons was used to measure the applied force and the displacement from which force-displacement curves were obtained to calculate the deformation work. In the case of impact loads, the pendulum was used with the Charpy (bending) and Izod (tensile) test to directly measure the deformation energy with impact loading. The results show that the strain energy absorbed under impact loading is significantly higher than under static loading. The reasons for this discrepancy are discussed in this paper.

Keywords: *Impact Load, Static Load, Tensile Load, Flexure, Energy Absorption.*

INTRODUCTION

The present research work proposes the demonstration of the energy conservation principle, that energy is neither created nor destroyed, but only transformed. In mechanics of materials, it is associated to the deformation energy produced in the materials at the moment of being submitted to mechanical tests carried out on brittle materials (up to breakage) and on ductile materials (in the plastic zone).

It is intended to demonstrate this law by means of mechanical tests with static loads and dynamic loads (Takeda, Kobayashi, 2023), and to compare the results of absorbed energy obtained to verify this principle, at first it was expected that both energies would be equal.

Theoretically, if there were no losses, the energy required to deform and fracture a steel specimen would be the same regardless of the loading rate. However, previous studies suggest that, "the maximum ultimate strength σmax, total elongation εt and absorbed energy Eab were found to increase significantly with increasing strain rate," (Meyers, Murr, 2012). This indicates that the energy absorption of a material tested under impact loading could differ from that observed under static loading.

The ability of the material to absorb energy depends not only on its composition and microstructural structure, but also on the type and rate of applied load, factors that significantly influence mechanical properties such as ultimate strength, ductility and energy dissipation (Zhang, Wang, & Chen, 2020).

The present investigation addresses this question by experimentally analyzing two types of structural steel under bending and tension, both under static and impact conditions. In a study, the mechanical work required to deform to failure ASTM A36 and A193 B7 steel specimens under these conditions was measured, the corresponding tests were carried out and it was verified that the results have considerable variations, so we proceed with the present research, where, in the first instance, the results of the tests and experimental calculations derived from these tests are presented.

A first scope is made to this question, the first conclusions are drawn; and, the possibility of a following analysis is left open, in which the different forms of energy are dissipated, this analysis can involve micro and macro issues, it should be analyzed from the part of movement of the atoms that generate heat and dissipating energy, to the external conditions of the tests such as speed of application of loads, heights, external climatic conditions, etc., and energy is dissipated in other forms, for example, heat by plastic deformation at the micro level, friction,

[1] Departamento de Ciencias de la Energía y Mecánica, Universidad de las Fuerzas Armadas ESPE, P.O. Box 171-5-231B, Sangolquí, Ecuador; egtapia2@espe.edu.ec.

[2] Departamento de Ciencias de la Energía y Mecánica, Universidad de las Fuerzas Armadas ESPE, P.O. Box 171-5-231B, Sangolquí, Ecuador; jeperez@espe.edu.ec.

remaining kinetic energy, etc., in order that the mentioned law is proved, and energy is dissipated in other forms, for example, heat by plastic deformation at the micro level, friction, remaining kinetic energy, etc. so that the mentioned law can be verified.

Several factors can influence the difference in energy absorbed under dynamic versus static loads. The loading rate can generate inertial effects, different deformation modes and different energy dissipation rates. Different studies have reported significant discrepancies in energy absorption associated with strain rate (Callister & Rethwisch, 2018; Meyers & Chawla, 2008). For example, impact loading (high velocity) tends to produce localized deformations and formation of energy-absorbing folds, while static loading (low velocity) tends to produce more uniform deformations (Lozano Pozuelo, 2013). As friction is encountered in the test system, it can also dissipate some of the energy in the form of heat; ideally, reproducible impact loading should minimize or equalize frictional conditions with respect to static loading to make the results comparable. At the microscopic level, rapid deformation (impact loading) can generate high dislocation densities, adiabatic shear bands or alternative deformation mechanisms that affect the energy absorbed before fracture (Lozano Pozuelo, 2013). It should be taken into account, boundary effects such as support or restraint conditions of the part can alter its failure mode under impact loading, redistributing the deformation energy in the system (Ledezma-Ramirez et al., 2019).

The objective of this article is to present an improved analysis of the energy discrepancies observed in steel under static and dynamic loads. In order to interpret the experimental results, bibliographic references describing the difference in energy behavior under static and impact loads will be integrated, taking into account factors such as velocity, friction, geometry, material properties, etc. Microstructural and boundary considerations are taken into account to give a comprehensive and useful technical explanation for the scientific community interested in knowing the energetic responses of the material under different types of loading.

Experimental Methodology

Materials

The materials used for the present investigation and to quantify the absorbed deformation energy in static and impact loads, were made in two types of steel and different configuration:

ASTM A36 low carbon steel square rod, see Figure 1, with width of 8.84 millimeters and height of 8.75 millimeters and length between supports of 102.9 millimeters.

Figure 1. ASTM A36 steel rod.

Threaded steel rods ASTM A193 B7 of 6.2 millimeters external diameter and 4.54 millimeters internal diameter with two nuts at each end, see figure 2, this type of rod was used to facilitate the fastening at the ends in the Charpy pendulum.

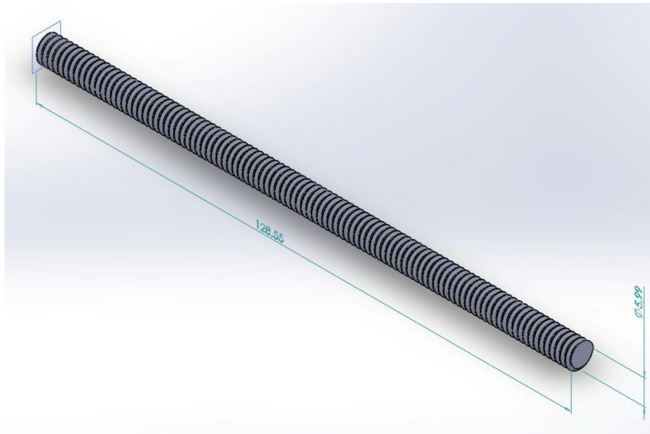

Figure 2. ASTM A193 B7 threaded rod.

King's foot of 300 millimeters range and 0.02 millimeters appreciation. Micrometer of 25 mm range and 0.01 millimeters appreciation, flexometer of 5 meters and 1-millimeter appreciation. Spreadsheet. It is important to mention that an important factor that can affect the results is the speed of the universal testing machine whose feed rate is 5 millimeters per minute. In the Charpy testing machine the impact speed is instantaneous.

For the static load tests, the AMSLER universal testing machine was used with a capacity of 10 tons, scales 1000, 2000, 5000 and 10000 kg, 1 kg appreciation, for specimens up to 40 cm in length. The testing machine allows the recording of the force vs. displacement curve, where static tension was performed on threaded rods and static bending on square rods as shown in Figure 3 and 4, force is measured in kilograms force and displacement in millimeters.

Figure 3. AMSLER universal testing machine.

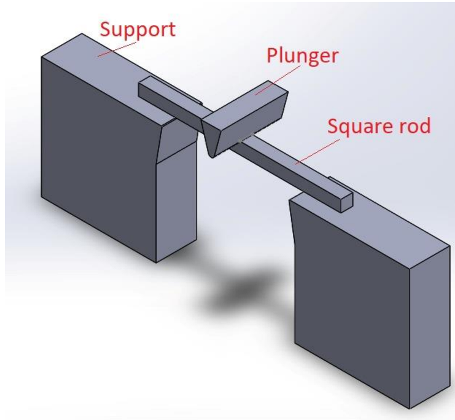

Figure 4. AMSLER Universal Flexure Testing Machine.

For the impact loading tests, a Charpy pendulum was used for bending for the A36 bars, using the standard Charpy single end-supported and center-struck (single beam test) setup, since the aim was to measure plastic strain energy rather than fracture toughness.

The same pendulum in Izod-type configuration was adapted for tensile impact testing, see Figure 4, used for A193 B7 threaded bars (impact tensile) by holding the ends of the threaded bar and applying a sudden pull-on release of the pendulum. The pendulum gave the energy absorbed in units of work, i.e. (kg-m).

The load application punch and the hardened steel supports were used in static bending and impact bending so that the tests were performed under the same initial geometrical conditions (position of supports, length of specimen). In addition, the influence of friction on the pendulum and its supports was minimized.

Figure 5. Charpy pendulum, bending.

The tests were performed for the elastic and plastic ranges. In the AMSLER universal testing machine, force and displacement are measured through sensors that transmit the signal to the control panel and deliver the results in the Excel database with the y-axis for force and the x-axis for displacement, a force vs displacement function is generated, to calculate the work, starting from the force vs displacement function

the calculation of a strain energy differential is given as $dU = F \cdot d\delta$,, integrating both terms we have $U = \int F \cdot d\delta$ (Riley et al. , 2001), applying this integral to the data provided by the Amsler universal testing machine, a small variation of the strain energy of the element is as shown in equation 1 (Chapra & Canale, 2015).

$$\Delta U_i = \left(\frac{F_i + F_{i+1}}{2}\right)(\delta_{i+1} - \delta_i) \qquad \text{Ec(1)}$$

Thus, the strain energy U of the element is as shown in Equation 2

$$U = \sum_{i=0}^{n} \left(\frac{F_i + F_{i+1}}{2}\right)(\delta_{i+1} - \delta_i) \qquad \text{Ec(2)}$$

The strain energy absorbed under static load was obtained by integrating the area under the force-displacement curve up to the point of maximum strain reached (equivalent to the mechanical work done on the specimen).

In Charpy's pendulum machine, which is based on the law of conservation of potential energy that is transformed into deformation energy for the breaking (tensile) or bending (flexural) of the elements, the measurement is direct using a potential energy difference. The value of the unit strain is defined as Epsilon (ε) and the expression for the calculation can be seen in equation 3 (Perez, 2023).

$$\varepsilon = \frac{L - Lo}{Lo} \cdot 100\% \qquad \text{Ec(3)}$$

Methods

In order to perform the tests, it was verified that the equipment is calibrated; this calibration is performed annually by INEN (Ecuadorian Institute for Standardization), with code C.ID: LMM 29, which ensures that the results obtained are reliable.

A certain number of tests were performed for each test:

- Tension in threaded rods with static loads: 6 tests.
- Tensile strength in threaded rods with impact loads (Izod): 6 tests.
- Flexure in square rods ASTM A36 steel with static loads: 5 tests.
- Flexure in square rods ASTM A36 steel by impact (Charpy): 5 tests.

It should also be verified that the load-free length in the tensile test and the length between supports in the bending test are measured with a tolerance of 0.02 millimeters. It should be verified that the temperature and humidity conditions are normal for the environment.

The calculations in the Charpy pendulum give a direct measurement from the scale of the machine, for the universal testing machine the measurement is indirect for which spreadsheets and the corresponding equations are used.

Results

The results presented below in each section indicate the average of several tests. The tensile test on rods was performed, the calculations of the work generated were made according to the equations shown in the experimental methodology section, the data shown below in Figures 4 are taken, then the calculations are made in the data sheet and the results are shown in the corresponding tables where “Lo” is the initial length of the specimen and “L” is the final length.

Tensile strength in threaded rods with static loads

The data shown in Table 1 are the result of 6 tests, these were obtained after performing the corresponding calculations from the information provided by the AMSLER equipment during the tensile test on threaded rods (see Figure 3).

Table 1. Result of Deformation Energy calculations U

Lo (mm)	L (mm)	(L-Lo) (mm)	Épsilon (%)	Energía /Energy (kg·m)
128,55	136,30	7,75	6,03	9,90

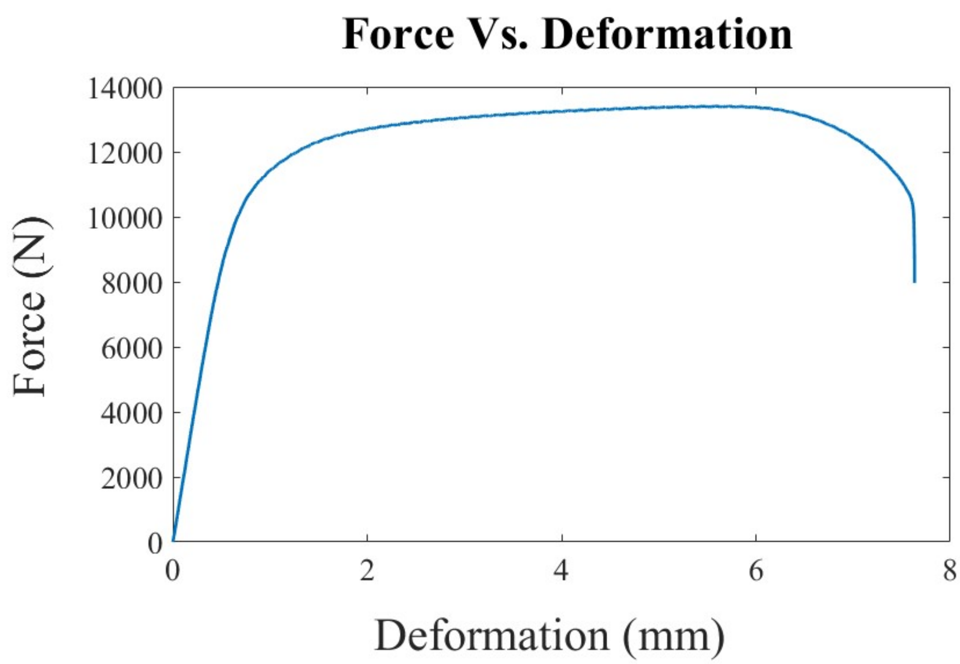

Figure 6. Machine data for threaded rod pulls

Tensile stress in threaded rods with impact loads (Izod)

The data shown in Table 2 is provided directly by the Charpy pendulum, the values shown are the average of 6 different tests.

Table 2. Deformation Energy calculation results U

Lo (mm)	**L (mm)**	**(L-Lo) (mm)**	**Épsilon (%)**	**Energy (kg·m)**
151,04	164,50	13,47	8,92	15,65

Flexure in square rods ASTM A36 steel with static loads

The data shown in Table 3 and Table 4 are the result of the calculations performed after obtaining the data curves as shown in Figure 6, and the results shown are the average of 5 different tests for the case of the results shown in Table 3 and of 3 different tests for the results shown in Table 4. Note that in Table 3 the test is performed on rods of 150 millimeters length, while in Table 4 the results are shown for tests performed on rods of 113 millimeters length, in the discussion section the results obtained will be analyzed.

Table 3. Deformation Energy U calculation results for 150 mm specimen.

Width (mm)	**Height (mm)**	**L Final (mm)**	**(L-Lo) (mm)**	**Energy (kg·m)**
8,87	8,77	157	7,6	14,1

Table 4. Deformation energy U calculation results for 113 mm specimen.

Width (mm)	Height (mm)	L (mm)	Energy (kg·m)
8,82	8,70	117,5	4,9

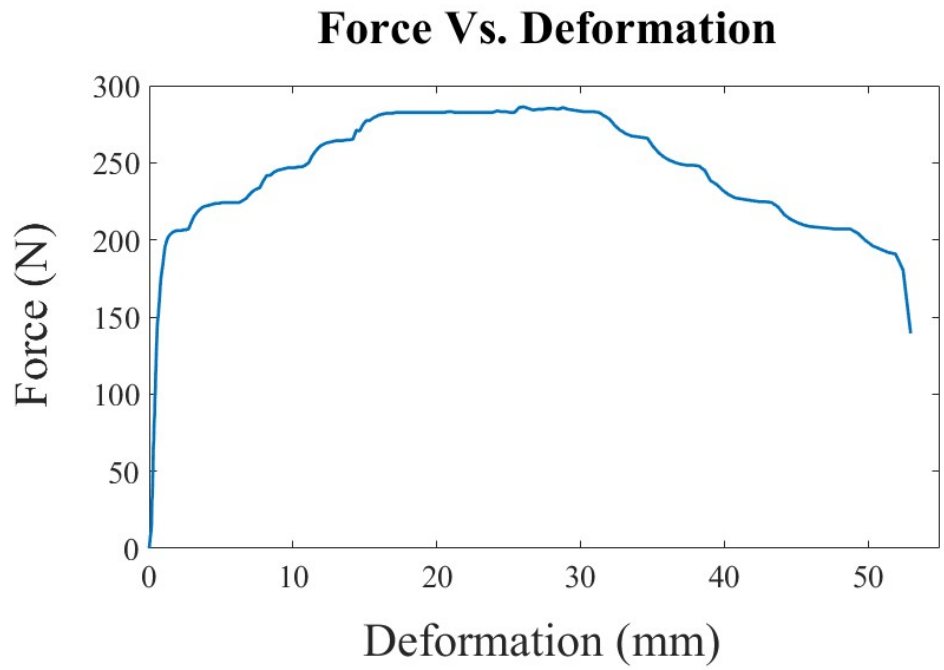

Figure 7. Machine data for bending on square rods

Flexure in square rods ASTM A36 steel by impact (Charpy)

Tests are performed on the Charpy Pendulum for two different lengths, for 150 mm length whose average results of 5 tests are shown in Table 5; and, for 113 mm length whose average results of 3 tests are shown in Table 6, being the length between supports 102.9 mm.

Table 5. Deformation Energy U calculation results for 150 mm specimen.

Width (mm)	Height (mm)	L Final (mm)	(L-Lo) (mm)	Energy (kg·m)
8,88	8,77	157,10	6,98	19,28

Table 6. Deformation Energy U calculation results for 113 mm specimen.

Width (mm)	Height (mm)	L1 (mm)	L (mm)	Energy (kg·m)
8,84	8,75	113,33	117,87	9,53

Micrographs

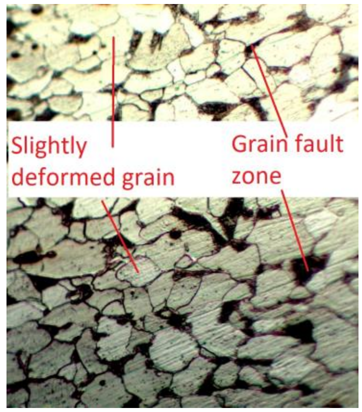

Figure 8. Static test micrographs 500 magnification

In the micrograph of A36 steel subjected to static bending, a slight plastic deformation in the grains is observed. The failure zones identified as "grain fault zone" suggest the beginnings of intergranular separation. There is no evidence of complete fracture, but moderate local deformation, reflecting the typical ductility of A36 structural steel (Leeco Steel, 2022).

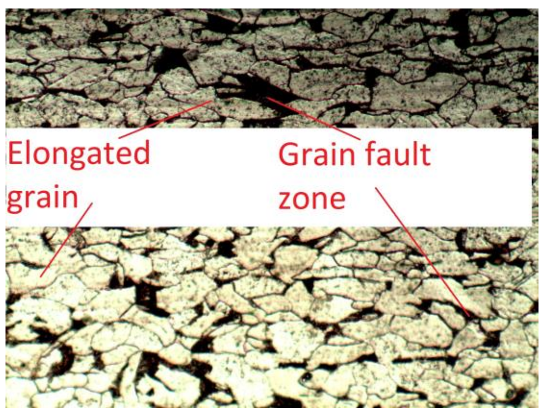

Figure 9. Charpy 500 magnification impact test micrograph.

The micrograph of the Charpy test shows deformation with grain elongation oriented in the direction of stress. Zones identified as "grain fault zone" are clearly observed, indicating areas of high stress concentration and small incipient cracks, but without full propagation, reflecting a typical more brittle response to rapid or dynamic loading (MacKenzie, 2020).

In all cases studied, the strain energy measured in the impact tests was found to be greater than that in the equivalent static tests. This was observed for both A36 members under bending and A193 B7 members under tension.

Quantitatively, for ASTM A193 B7 bars subjected to tension, the strain energy to fracture in the impact test was approximately 1.6 times the energy absorbed under equivalent static load. The results were consistent in repeat tests, showing that the phenomenon is reproducible. It should be noted that the differences were mainly manifested in the plastic range of the deformation, since in the initial elastic range both curves (static and impact) coincide to a large extent, which was expected, since the linear elastic behavior depends mainly on the material and geometric stiffness.

Another result was the observation of a higher unit strain in the tensile specimens under impact compared to the static ones. That is, the bars subjected to impact tensile experienced a slightly higher elongation before fracture than the statically loaded ones.

These quantitative results confirm an important discrepancy: the energy required to deform and fracture the steel was higher under impact loading than under slow static loading under the same geometrical conditions. The possible causes are discussed below and this behavior is compared with findings from other materials and studies.

Discussion

The tests performed show that the steel specimens absorbed more strain energy during the impact tests than in the static tests. The comparison of the results of the average Deformation Energy calculated between static tensile (9.9 kg-m) and impact tensile (15.7 kg-m) differ significantly, this is the beginning of the problem raised since, based on the law of conservation of energy, these values should be equal. By calculating the Epsilon value, it can also be verified that the Energy values are different, maintaining the initial trend, i.e., that Epsilon is higher in the impact load test, the same happens for static loads.

It can be seen in Table 7 that the relationship between these energies remains between 1.4 and 1.9, which indicates that the impact energy is higher than the energy in static test.

Table 7. Static Vs Impact Deformation Energy Ratio

	IMPACT	STATIC	RATIO OF U IMPACT VS. U STATIC
TENSION IN THREADED RODS	15,65	9,9	1,6
BENDING IN 150 MM ROD	19,28	14,1	1,4
BENDING IN 150 MM ROD	9,53	4,9	1,9

Entre varillas de 150 milímetros y de 113 milímetros se puede ver que está incluida la energía que genera la fricción de la varilla con la cara de los apoyos, de tal manera que cuando se baja la distancia entonces la energía es menor. En la tabla 8 se muestra la diferencia del trabajo generado por la fricción para carga estática y para carga de impacto, se puede verificar que los valores son similares por lo que se concluye que la diferencia efectivamente se trata del trabajo por fricción en cada caso.

Table 8. Diferencia de Trabajo debido a fuerza de fricción.

Strain Energy	Work with static load	Work with impact load
150mm Steel rod	14,1	19,28
113mm Steel rod	4,9	9,53
Difference	9,2	9,75

There is an energy difference that is dissipated in various other forms of energy such as heat, potential, kinetic, vibrational, air resistance, friction. Several factors contribute to this difference:

Effects of loading velocity and inertia: Under impact loads, the sudden application of force generates stress waves and inertial effects along the specimen. This leads to deformation not occurring uniformly or statically, but parts of the specimen may experience intense localized plastic deformation that dissipates more energy. Previous studies show that in thin structures subjected to axial impact have similar behaviors: the higher the impact velocity, the more localized collapse occurs, which alters the energy absorbed and is. Lozano (2013) found that increases in impact velocity can change the deformation mode of thin tubes from global buckling to multiple local buckling, increasing plastic energy dissipation.

Deformation hardening and strain rate: The steels studied, being ductile materials, exhibit some degree of strain rate sensitivity. At higher loading rates, the dislocation motion mechanisms have less time to reorganize, which typically results in an increase in the apparent strength of the material. As a result, the material can withstand higher loads before fracturing under impact, absorbing more energy in the process.

Conversion of energy into dissipation heat: In a slow static test, much of the plastic deformation work is gradually dissipated as heat that is transferred to the environment, maintaining nearly local isothermal conditions. In contrast, in an impact deformation occurs so rapidly that the process is almost adiabatic, i.e., the heat generated by plastic deformation does not immediately diffuse out of the deformed zone. This can raise the local temperature in the deformation zone, causing thermal softening of the steel. While thermal softening may reduce strength momentarily, the rate hardening effect and inertia tend to dominate at moderate impact scales, resulting in distinctly greater energy absorbed for fracture.

Friction and boundary conditions: In the tests performed, friction was controlled so that it did not introduce appreciable differences between the static and impact cases (for example, the supports in bending were the same, and in tension the configuration avoided friction). In the tests performed the boundary conditions remained constant between static and dynamic, the differences in other contexts (change of boundary conditions) could be amplified or reduced if the constraints change by increasing or decreasing the energy absorption changing the result of the work.

The higher energy absorbed on impact is consistent with a more dynamic response: higher instantaneous strength of the material, more concentrated plastic deformation. In contrast, under static loading the material flows more stably and a portion of the external work can be returned as recoverable elastic energy or dissipated gradually without requiring as much energy to reach fracture.

The results show significant differences in energy absorption between static and dynamic loads. The energy absorbed during impact loads was higher with respect to static loads. This behavior is congruent with previous research where it is mentioned that rapid plastic deformation and inertia (impact loading) generate higher energy absorption in dynamic conditions (Lozano Pozuelo, 2013; Meyers & Murr, 2012).

In the static tensile test, the test is performed slowly, giving way to the movement of electrons inside the material which generates heat and therefore dissipation of energy in the form of heat, on the other hand, in the impact test in which the deformation occurs in a very short time, no time is given for heat energy to be generated, which would explain the fact that the energy results for impact loads are higher. This hypothesis can be verified in further research work.

Design And Engineering Implications

The finding that the dynamic deformation energy in these steels is higher than the static one has important consequences. It is vital for strength that in the calculation, one of the steps prior to execution, only a static property, such as the value of the absorption energy resulting from a gradual tensile test, is considered thinner than in reality. For this reason, engineering regulations and procedures include special elements or techniques for impact loads. A common tactic is to use equivalent static loads to symbolize an impact: in other words, set a static load or energy that produces impact-like effects and design for such a situation (Kumar et al., 2024).

Lann and Nilsson (2015) discuss techniques for transforming impact spectra into equivalent static loads, making it easier for engineers to evaluate structures under impacts without the need to explicitly simulate the entire event. This is particularly beneficial in initial evaluations. However, for critical structures, dynamic simulations or direct impact tests are often carried out. For example, in the automotive sector, the crash test cannot be replaced to verify vehicle impact performance, since it covers all the real elements of energy absorption (materials, geometries, failure modes). Likewise, in seismic-resistant design, pseudo-dynamic tests or tests with high cyclic load histories are used to ensure that the structure will dissipate earthquake energy without collapse.

The present research also evidences the relevance of design elements that optimize energy harvesting. An illustrative case is that of roll cages in competitive vehicles: research by Rockwood Iglesias (2024) showed that adding reinforcements in critical areas of the cage increases the distributed plastic deformation and optimizes energy absorption in the event of an impact, providing greater protection to the occupants.

This evidences a fundamental principle: to orient the deformation towards areas or elements capable of dissipating energy in a regulated manner.

CONCLUSION

Conclusions

- The impact deformation energy for tensile and bending is higher with respect to static
- The work due to frictional force in bending is equal in both cases, for both static and impact.
- The unit deformation in impact tensile is higher than for static.
- In static and impact tensile, there is no friction, so the results are directly the tensile strain energy.
- It can be seen that the deformation energy due to static loads shows a marked difference with respect to the tests performed with impact loads, this is due to the fact that the energy is dissipated in other forms of energy such as heat, friction, kinetic energy, etc.

In conclusion, the energy discrepancies observed do not point to contradictions in the law of conservation of energy, but rather point to complex pathways of energy dissipation and storage in a material for different loading modes. This knowledge has repercussions in the design of structural and mechanical components that are under the action of impacts, shocks or short duration loads: not only the design for equivalent static loads has to be considered, but the dynamics of the event has to be included for a safe performance. We would propose to move the research focus to post-test microstructural analyses along with explicit nonlinear numerical modeling to further quantify energy partitioning (e.g., quantify how much of the impact energy is transformed into heat, creation of new fracture surfaces or homogeneous plastic deformation). Ultimately, this work reinforces the notion that the energetic behavior of materials is multifaceted and dependent on the rate of loading, the significance of which becomes crucial for advances in materials and structural engineering.

REFERENCES

Callister, W. D., & Rethwisch, D. G. (2018). Ciencia e ingeniería de materiales (10ª ed.). Wiley.

Gettys, E., Keller, F., & Skove, M. (2005). Física para ciencias e ingeniería (Tomo I, 2ª ed.). McGraw Hill.

Pérez, J. (2023). Mecánica de Materiales (1ª ed.). Instituto Ecuatoriano de Propiedad Intelectual. ISBN: 978-9942-44-068-6.

Chapra, S. C., & Canale, R. P. (2015). Métodos numéricos para ingenieros (7ª ed.). McGraw-Hill Education.

Meyers, M. A., & Murr, L. E. (2012). Shock wave and high-strain-rate phenomena in metals: Concepts and applications. Springer.

Meyers, M. A., & Chawla, K. K. (2008). Mechanical Behavior of Materials (2ª ed.). Cambridge University Press.

Riley, W., Sturges, L., & Morris, D. H. (2001). Mecánica de materiales. Limusa Grupo Noriega Editores.

Kumar, R., Sharma, P., & Singh, A. (2024). Review on comparison of energy absorption in steel fibre reinforced concrete, polypropylene fibre reinforced concrete, hybrid fibre reinforced concrete. International Scientific Research Journal, 12(1), 15–24.

Ledezma-Ramírez, D. F., Tapia-González, P. E., & Castillo-Morales, M. (2019). Análisis del efecto de las condiciones de frontera en la respuesta dinámica de placas anisotrópicas. Revista de Ingeniería Estructural, 15(2), 125–134.

Zhang, X., Wang, H., & Chen, Y. (2020). Rate-dependent deformation and fracture of structural steels under dynamic loading. Engineering Fracture Mechanics, 235, 107–176. https://doi.org/10.1016/j.engfracmech.2020.107176

MacKenzie, D. S. (2020). Four basic types of fracture mechanisms. Gear Solutions Magazine.

Lozano Pozuelo, J. (2013). Mecanismos de absorción de energía en estructuras de pared delgada sometidas a impacto axial: el papel de la inercia y el endurecimiento por deformación [Tesis de máster, Universidad Carlos III de Madrid].

Zhao, L., Cheng, B., & Tan, S. (2023). Comparative performance of composite sandwich panels and non-composite panels under blast loading. Proceedings of the 7th International Conference on Protective Structures (ICPS7), 563–570.

Rockwood Iglesias, R. E. (2024). Diseño de una jaula antivuelco para un vehículo de competencia utilizando técnicas de ingeniería asistida por computador (CAE) [Tesis de grado, Universidad del Azuay]. https://dspace.uazuay.edu.ec/bitstream/datos/14112/1/19635.pdf

Lann, J., & Nilsson, M. (2015). Evaluation of equivalent static load methods for crash analysis. Lund University Publications.

Leeco Steel, LLC. (2022). ASTM A36 comparada con ASTM A572.Recuperado de https://www.leecosteel.com

Takeda, N., & Kobayashi, A. (2023). High velocity tensile properties of Ti-15V-3Cr-3Al-3Sn alloys. Elsevier. https://doi.org/9781003418146-7